MODELLING AND IDENTIFICATION OF NONLINEAR DYNAMIC LOADS IN POWER SYSTEMS

Daniel Karlsson
Sydkraft AB, S-20509
Malmö, Sweden

David J. Hill, Senior Member
The University of Newcastle,
Callaghan, NSW 2308, Australia

Abstract

This paper describes an approach for experimental determination of aggregate dynamic loads in power systems. The work is motivated by the importance of accurate load modelling in voltage stability analysis. The models can be expressed in general as nonlinear differential equations or equivalently realised in block diagram form as interconnections of nonlinear (memoryless) functions and linear dynamic blocks. These components are parameterised by load indexes and time constants. Experimental results from tests in Southern Sweden on the identification of these parameters are described.

Keywords

Load modelling, power systems, dynamics, voltage stability.

1 Introduction

Models for dynamical analysis of power systems typically have a consistency problem. While it is scientifically possible to give quite detailed models for generators, lines, transformers and control devices, load modelling can often only be treated on an ad hoc basis. In stability analysis for instance, we need a representation of effective power demand at high voltage buses. This may include the aggregate effect of numerous load devices such as lighting, heating and motors plus some levels of transformer tap-changing and other control devices. Building up the aggregate effect by combining device characteristics may not be possible. In many cases, quite simplified aggregate load representations like impedances are used alongside detailed generator models. This seems related to three research questions:

1. To what extent are accurate load models important in power system stability analysis;

2. Given that derivation of aggregate models from component characteristics is not feasible, what are appropriate mathematical structures to represent high voltage effective load;

3. How can the aggregate load models (from question 2) be determined in practice.

Briefly, we refer to these questions as model justification, structure determination and identification respectively. The present paper is primarily concerned with model structure and identification from system tests.

The study of load model justification in dynamical analysis of power systems seems to demand more attention. The usual aggregate load model expresses the real and reactive load powers as nonlinear functions of voltage; for instance, the form $P_0\left(\frac{V}{V_0}\right)^a$ with a single index a, for real load power is popular (with a similar form for reactive power) [1–3]. Frequency dependence can be included, but is usually ignored. For transient (angle) stability, there is still some debate about whether acceptable first swing assessment can be done with impedance load models, i.e. $a = 2$ rather than specifically determined values [4–6]. The present work is motivated more by voltage stability analysis [7]. Here it is widely accepted that load characteristics at low voltage play an important role; further, dynamics of loads is important [7, 8]. However, the dynamical description of loads at HV buses certainly required more attention. For static (load flow) voltage stability analysis, it is often assumed that the load powers are in fact constant, i.e. $a = 0$, in

order to reflect voltage control action by tap-changers and switched capacitance. This is not appropriate in the study of dynamic behaviour.

This paper is an outcome of projects in Sweden aiming to develop dynamical load models and study voltage dynamics following large disturbances. A study of dynamical load modelling was initiated by Karlsson and Pehrsson [9]. Walve [8] commented on their model while discussing the importance of load modelling in understanding the 1983 Swedish blackout. The model in [9] included a dynamic voltage term within a linear structure. Observations of field load transient responses led Edström and Walve [10] to study in more detail some nonlinear aspects of load recovery following a voltage step. Although voltage collapse in general is a phenomenon that takes several minutes, it was recognized that most of the load modelling work so far had concentrated on induction machines in the range of seconds after a disturbance. The aim was to develop accurate load models for voltage stability studies, valid for at least several minutes after a disturbance. However, at this stage no (nonlinear) model relating general voltage to power signals was proposed. Hill [11] proposed such a model with a simple nonlinear structure defined by two nonlinear functions and a recovery time constant. This was subsequently used to explore static vs dynamic aspects of voltage stability [12–14]. Meanwhile Karlsson et. al. devised experiments to record load responses to various voltage signals [15]. This data was used to identify a particular recovery model which can be derived from the general input–output dynamical model described earlier in [11, 12].The load functions were assumed to have the single index form. This paper aims to present a coordinated discussion of the overall load modelling approach covering model structures and parameter identification. The discussion of structures blends ideas presented previously by Hill [11, 13] and Karlsson [15]; results from the recent thesis by Karlsson [16] are used to illustrate model parameter identification from field tests.

The structure of the paper is as follows. Section 2 discusses typical load responses and their representation as solutions of nonlinear differential equations. These can be expressed in higher-order scalar or first-order vector form. It is also convenient to view the models as block diagram interconnections of nonlinear functions and linear dynamic blocks. Section 3 reviews techniques for parameter identification in nonlinear systems. Section 4 follows Chapter 3 of the thesis [16] to illustrate recovery model identification from field tests; a one dimensional model with single index steady-state and transient load functions is identified for data reflecting seasonal variation.

2 General Load Model Structures

Consider a high voltage bus as in Figure 2.1. The real and reactive power demands P_d and Q_d are considered to be dynamically related to the voltage V.
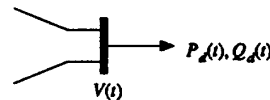
Figure 2.1 High Voltage Load Bus

Measurements in the laboratory and on power system buses [9, 10, 17] show that the load response to a step in voltage V is of the general form shown in Figure 2.2. (The responses for real and reactive power are similar qualitatively; only the real power response is shown.) The significant features of the response are as follows: 1) a step in power immediately follows a step in voltage; 2) the power recovers to a new steady-state value; 3) the recovery appears to be of exponential (sometimes underdamped) form, at least approximately; 4) the size of the step and the steady-state value are nonlinearly related to voltage [10]. These features are easily connected to physical aspects of specific loads [13].

158
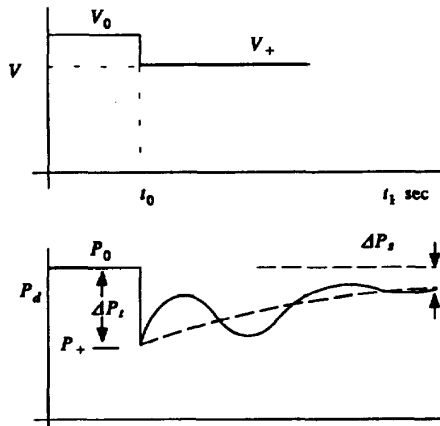
Figure 2.2 General Load Response

As in [13], we can propose a general load model as an implicit differential equation

$$f(P_d^{(n)}, P_d^{(n-1)}, ..., \dot{P}_d, P_d, V^{(m)}, V^{(m-1)}, ... \dot{V}, V) = 0 \qquad (1)$$

where $P_d^{(j)}, V^{(i)}$ denote the higher order derivatives of P_d, V respectively. (A similar equation applies for reactive power Q_d.)

For first order dynamics, equation (1) becomes

$$f(\dot{P}_d, P_d, \dot{V}, V) = 0 \qquad (2)$$

An input - output version of this model is illustrated simply in Figure 2.3 where V is chosen as the input to a nonlinear dynamical system with output P_d.
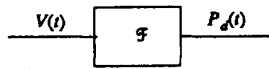
Figure 2.3 Input - Output Load Representation

The above discussion of Figure 2.2 suggests there are (at least) two nonlinearities in a reasonable model; one describing a steady-state relationship, i.e. the steady-state offset ΔP_s, and the other a transient one, i.e. the jump ΔP_t. Further linear dynamics can approximately describe the transient recovery. Assuming first order dynamics, Hill [11] proposed that the load response in Figure 2.2 can be regarded as the solution of the scalar differential equation

$$T_p \dot{P}_d + P_d = P_s(V) + k_p(V)\dot{V} \qquad (3)$$

The motivation for this structure is easy to see.

Setting derivatives to zero gives the steady-state model

$$P_d = P_s(V) \qquad (4)$$

Rewriting (3) as

$$T_p \frac{dP_d}{dt} + P_d = P_s(V) + T_p \frac{d}{dt}(P_t(V)) \qquad (5)$$

where

$$P_t(V) := \frac{1}{T_p} \int_0^V k_p(\sigma)d\sigma + c_0 \qquad (6)$$

c_0 a constant, clearly shows that $k_p(\cdot)$ defines the fast changes in load according to $P_d = P_t(V)$. (The presence of T_p in (6) can be avoided by replacing $k_p(V)$ by $T_p Q_p(V)$ in (3).) To see this precisely, we consider the step response in Figure 2.2.

For solving equation (3) analytically [11, 13] or numerically [12], the fact that all solutions satisfy an equivalent normal form model was used. This form is expressed (with slight change of notation to [11-13]) as

$$\dot{x}_p = -\frac{1}{T_p}x_p + N(V) \qquad (7)$$

$$P_d = \frac{1}{T_p}x_p + P_t(V) \qquad (8)$$

where

$$N(V) := P_s(V) - P_t(V) \qquad (9)$$

The solution of differential equation (3) for the voltage step is

$$P_d(t) = P_t(V_+) + [P_s(V_0) - P_t(V_0) - P_s(V_+)]$$
$$+ P_t(V_+)] \quad e^{\frac{-(t-t_0)}{T_p}}, t > t_0 \qquad (10)$$

Note

$$P_d(t_0 -) = P_s(V_0)$$
$$P_d(t_0 +) = P_s(V_0) - [P_t(V_0) - P_t(V_+)] \qquad (11)$$
$$P_d(\infty) = P_s(V_+)$$

From these observations, we easily obtain for power increments shown in Figure 2.2

$$\Delta P_t := P_d(t_0 -) - P_d(t_0 +) = P_t(V_0) - P_t(V_+) \qquad (12)$$
$$\Delta P_s := P_d(t_0 -) - P_d(\infty) = P_s(V_0) - P_s(V_+) \qquad (13)$$

So the nonlinear functions $P_s(\cdot)$ and $k_p(\cdot)$ (or $P_t(\cdot)$) independently determine the steady-state and transient power increments ΔP_s and ΔP_t respectively.

In choosing a model to fit field data [15], Karlsson chose to use this normal form structure (7)-(9). To explore the first order case in detail, it is convenient to rewrite it in his more physically suggestive notation by setting $x_p = T_p P_r$

$$T_p \dot{P}_r + P_r = N(V) \qquad (14)$$
$$P_d = P_r + P_t(V) \qquad (15)$$

We will see some physical significance of P_r below. The model used in [15, 16] is expressed in the form (14), (15), (9) with the special load functions:

$$P_s(V) := P_0 \left(\frac{V}{V_0}\right)^{a_s} \qquad (16)$$

$$P_t(V) := P_0 \left(\frac{V}{V_0}\right)^{a_t} \qquad (17)$$

The steady-state model $P_d = P_0 \left(\frac{V}{V_0}\right)^{a_s}$ corresponds to the widely used static model [1-3]. Note that in model form (3), (17) corresponds to $k_p(V) = T_p \frac{dP_t}{dV} = T_p a_t \frac{P_0}{V_0} \left(\frac{V}{V_0}\right)^{a_t-1}$.

We will continue here with the more general form (14) - (15). Two separate functions appear, namely $P_s(\cdot)$ associated with steady-state voltage dependence and $P_t(\cdot)$ associated with transient voltage dependence. In principle, these could be chosen with various polynomial forms [3].
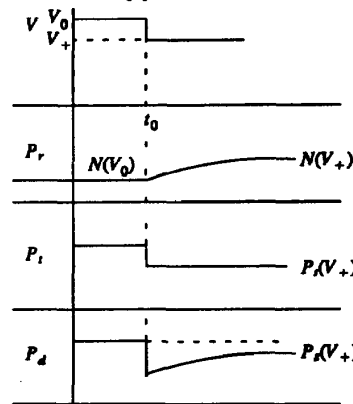
Figure 2.4 Decomposition of First-Order Recovery Response

It is instructive to note how the recovery response arises from the model in form (14) - (15). This is shown in Figure 2.4 for the step response. Clearly, $P_t(\cdot)$ describes the transient jump and state variable P_r the recovery to a steady-state determined by $P_s(\cdot)$.
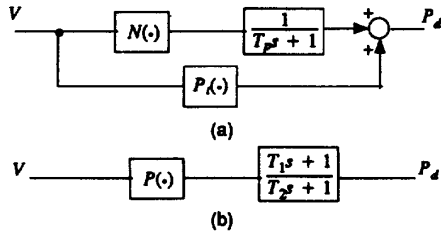
Figure 2.5 Block Diagram Representations of First-order Load Model

Now, it is convenient to note that the normal form model is easily given the block diagram representation shown in Figure 2.5 (a). One special case of interest is where the steady-state and transient load functions are related by constant scaling, i.e. $P(V) := P_t(V) = CP_r(V)$. Then the block diagram can be simplified considerably. From (5), we get

$$T_p \dot{P}_d + P_d = P(V) + \frac{T_p}{C}\frac{dP(V)}{dV}$$

The corresponding block diagram is shown in Figure 2.5 (b) with $T_1 = \frac{T_p}{C}, T_2 = T_p$. A reviewer of [13] pointed out that this model has been used in utility software. It captures recovery behaviour, but does not allow separate indices for transient and steady-state behaviour.

In summary, it is now clear that the scalar nonlinear load model and its equivalent normal form (14), (15), (9) (or (7) - (9)) can be viewed as a block diagram interconnection of nonlinear functions and a linear transfer function in the general form of Figure 2.6 [18]. Analytical aspects of this generalisation are pursued in [18].
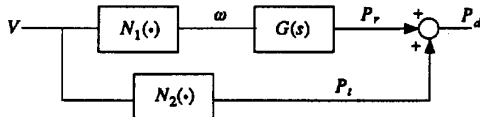
Figure 2.6 General Load Model

For higher order dynamics

$$G(s) = \frac{b_m s^m + b_{m-1} s^{m-1} + \dots + b_0}{s^n + a_{n-1} s^{n-1} + \dots + a_0} \qquad (18)$$

the response of Figure 2.2 can be obtained with more exotic recovery, i.e. multiple time-constants and/or oscillatory behaviour.

The first-order normal form (14)–(15) (or (7)–(9)) is a special case of more general representation. Translating the transfer function $G(s)$ to an equivalent state-space representation [19] gives

$$\dot{x}_p = Fx_p + Gw$$
$$P_r = H^T x_p \qquad (19)$$

where x_p is an n-dimensional vector and F, G, H are appropriately dimensioned matrices. Combining (19) with

$$\omega = N_1(V) \qquad (20)$$
$$P_t = N_2(V) \qquad (21)$$
$$P_d = P_r + P_t \qquad (22)$$

from Figure 2.6 gives

$$\dot{x}_p = Fx_p + GN_1(V)$$
$$P_d = H^T x_p + N_2(V) \qquad (23)$$

This model structure is an n-dimensional generalisation of the one-dimensional case described by (7)–(9); there the matrices F, G, H are scalars. In [18] it is seen that a second order $G(s)$ gives responses close to those reported in Shackshaft et. al. [17] by appropriate choice of parameters $a_0, a_1, b_0, b_1, a_r, a_t$ (and reactive counterparts).

The model (23) can be easily incorporated into simulation programs for power system dynamics. The parameters which determine matrices F, G, H and nonlinear functions $N_1(\cdot)$ and $N_2(\cdot)$ must be obtained from measured data.

3 Parameter Estimation Methods for Nonlinear Systems

The load model (23) has the form of nonlinear system

$$\dot{x} = f(x, u, \theta)$$
$$y = g(x, u, \theta) \qquad (24)$$

where θ denotes the parameters to be estimated; in this case, the components of F, G, H and coefficients in nonlinearities $N_1(\cdot)$ and $N_2(\cdot)$.

We now look at identification of such models, i.e. estimation of the parameters θ. In practice, there could be numerous parameters. There are ways to reduce the number:

i)   Use of canonical forms [18] for (F, G, H) reduces the number of parameters in (23) to $n + m$;

ii) Use of special structures in $N_1(\cdot)$ and $N_2(\cdot)$, e.g. the single-index forms (16)–(17).

For the first-order model (14)–(17), we have the five parameters P_0, V_0, a_s, a_t, T_p.

For general systems of the form (24), we can proceed as follows. Suppose that we have measurements of outputs and inputs at N time instants, $y(t_k)$ and $u(t_k)$ $k = 1, ..., N$. Based on these measurements, we want to obtain estimates of the parameter vector θ. There are different approaches at hand, depending on what further assumptions of the model are made.

The simplest approach is to adopt the model (24) as is, without further assumptions. The system is then simulated using the inputs $u(t_k)$, i.e. the differential equation (24) is solved using some kind of algorithm for numerical integration. The simulated outputs $\bar{y}(t_k)$ so produced are then compared to the actual measured outputs $y(t_k)$. Typically a least squares quadratic criterion is formed

$$V_N(\theta) = \sum_{k=1}^{N} (y(t_k) - \bar{y}(t_k))^2. \qquad (25)$$

This criterion is minimised using some optimisation algorithm. Obviously this is going to be computationally burdensome. For every step in the optimisation, the integration routine has to be run a number of times to produce the function value V_N and to obtain a numerical gradient of V_N with respect to θ.

An obvious disadvantage with the deterministic model (24) is that all anomalies in data have to be captured by the parameters. A way to circumvent this is to introduce noise in the model description and estimate them by a maximum-likelihood criterion [20].

The stochastic model leads to even more computations than the deterministic one, but can be more effective. The deterministic approach is straight forwardly carried out with MATLAB curve fitting commands. An important input to such programs, besides the data, is an initial parameter estimate $\theta(0)$. This can often be obtained from special response tests like steps and ramps. A good initial estimate can prevent the problem with nonlinear optimisation where the estimate can get stuck in a local minimum.

Another important issue is identifiability [21]; the data must be 'rich enough' to enable computation of the parameters. More complex models with a higher number of parameters require data with more information content.

4 Results from Field Measurements

Some results from [16] are used to illustrate identification of the nonlinear recovery models. The load models derived are intended to represent the temporary load-voltage characteristics on a time scale of about 10 seconds to 10 minutes. These models are derived especially for voltage stability studies. A high load-voltage sensitivity will generally help the system to survive, after a reduction of the supply voltage, by means of reduced power consumption. The power consumption in the stressed system, in the range of a few seconds to about 10 minutes, is therefore of great interest, as well as the impact of the automatic on-load tap-changer (OLTC) control.

4.1 Field Measurement Recordings

Field measurements from two substations in Southern Sweden with different load compositions are presented in this section. Recordings were taken both in wintertime (February, 1991), with a large part of the load consisting of electrical home heating appliances, and in the summer (June and August, 1991) when the amount of electric heating is small. The load demand profile was studied in

order to perform the tests during periods with small random variations of the load. (Recall the discussion in Section 3.) The outdoor temperature was around 0°C in February, 10°C in June and about 18°C in August. The supply voltage, as well as the active and reactive power, was recorded on the secondary side of the step-down transformers. The supply voltage is defined on the transformer secondary side (10 or 20 kV), as shown in Figure 4.1. To evaluate the voltage applied to the actual load devices, the voltage drop in the distribution system, including one or two additional transformers with fixed ratios, has to be taken into account.
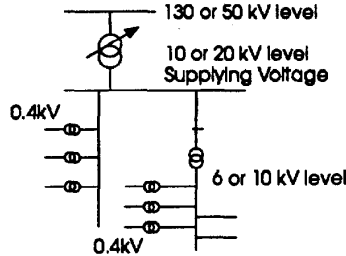
Figure 4.1. The supplying voltage is defined on the second side of the step-down transformer, connected to a 130 or 50 kV system on the primary side.
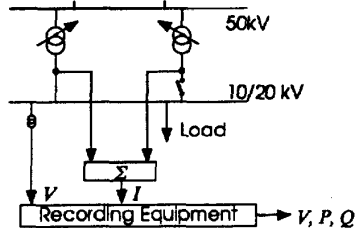
Figure 4.2. Arrangements for the step-change recordings. The two tap-changers are set at different positions and the circuit-breaker for one of the transformers is used to form the step.

Fotevik (FVK), one of the load areas studied, consists mainly of electrically heated houses, and the other one, Svedala (SLA), is a combination of standard homes and industries. All OLTC's between the feeding substation and the actual load devices were blocked during the tests. No shunt or series capacitors were in operation neither in the FVK area nor in the SLA area, during the tests. In FVK, the measurements were taken on the secondary side of two parallel 25 MVA, 50/20 kV transformers. The load was fed by a 20 kV system (cables – 35 km, and overhead lines – 17 km), a 10 kV system (cables – 63 km), 3 substations rated 20/10 kV, and 47 and 85 transformers rated 20/0.4 kV and 10/0.4 kV, respectively. The load was around 30 MW in February, about 18 MW in June and 10 MW in August.
In SLA, the measurements were taken on the secondary side of two parallel 16 MVA, 130/10 kV transformers, supplying both the homes and industry. The load was fed by a 10 kV system (cables – 42 km, and overhead lines – 55 km) and 108 transformers rated 10/0.4 kV. The load was around 15 MW in February, about 10 MW in June and 9 MW in August.
A voltage magnitude ramp variation was applied in the two substations in February and step-changes were used in June and August. The ramp was obtained by simultaneous manual change of the tap-changer positions on the two transformers operating in parallel. The tap-changer positions were changed as fast as possible (about 8 seconds per step) from the highest to the lowest acceptable position (i.e., the highest and lowest acceptable voltage magnitudes on the transformer secondary side) and vice versa. The number of steps between the highest and lowest acceptable tap-changer positions varied from 5 to 7. Each step corresponds to 1.67% of the rated voltage on the transformer low voltage side. A ramp formed in this way is, of course, an approximation consisting of many subsequent step-changes. The load demand level was too high in February to permit single transformer operation in FVK and SLA and, therefore, the step-change could not be applied at that time.
True step-changes in the supplying voltage magnitude were obtained by operating the two transformers in parallel at different tap levels, and then switching off/on the circuit-breaker for one of the transformers, see Figure 4.2. This method of forming a step-

change has also been used in [17] but the recording time was just a few seconds.
The voltage magnitude variations are shown in Figure 4.3.
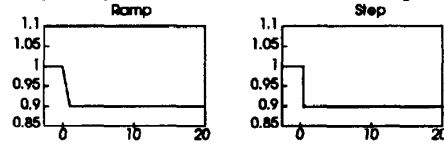
Figure 4.3 Basic shapes of the voltage magnitude variations applied in the two substations; ramp, step

For all the recordings, the transformer with the highest tap position was switched. Voltage steps of ±5 to 10% were obtained in this way. The limit for the size of the voltage step was set by the voltage level on the transformer secondary side (the voltage feeding the load), the amount of reactive power circulating in the two transformers and the secondary voltage level of the unloaded transformer.
The results were quite similar for the two substations and there were no major differences in the basic response at different times of the day. However, there was a significant reduction in the amount of active power recovered as the outdoor temperature increased. For some of the summer measurements there was hardly any recovery at all.
The diagrams in Figure 4.4, for February recordings, show that the active power will start to increase as soon as the voltage reduction stops. Within about five minutes, half of the initial active power reduction has been recovered. Initially, the composite load is almost equal to a constant impedance load. Finally, the active power curve stabilizes between constant current and constant power. The small increase in reactive power after the voltage reduction originates from the increased reactive losses due to the increased current, when the active power recovers at lower voltage.
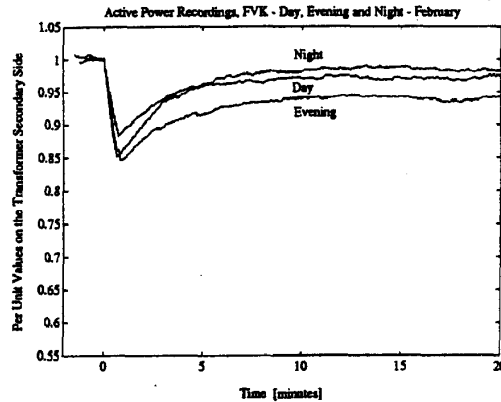
Figure 4.4a. Active power recordings after a voltage reduction in FVK
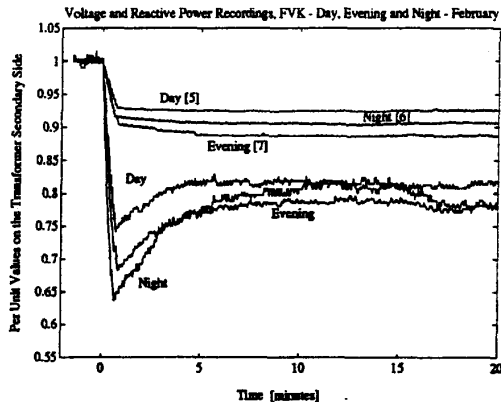
Figure 4.4b. Voltage and reactive power recordings after a voltage reduction in FVK; February; day, evening and night. The number of tap-changer steps used for the ramp is shown in brackets.
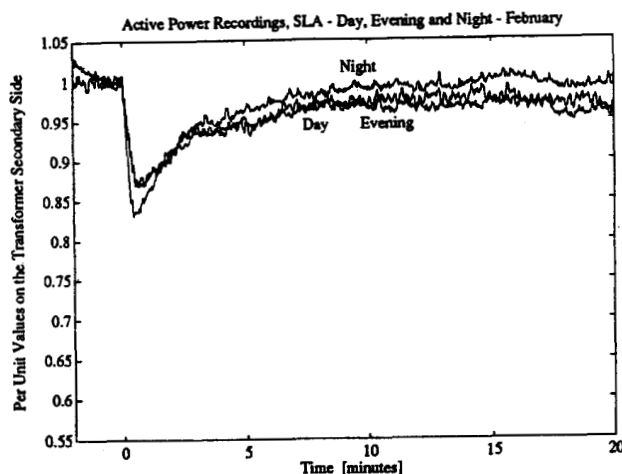
Figure 4.4c. Active power recordings after a voltage reduction in SLA
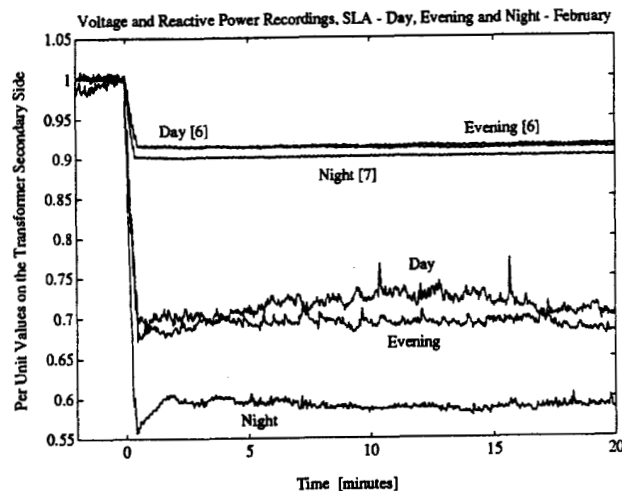
Figure 4.4d. Voltage and reactive power recordings after a voltage reduction in SLA
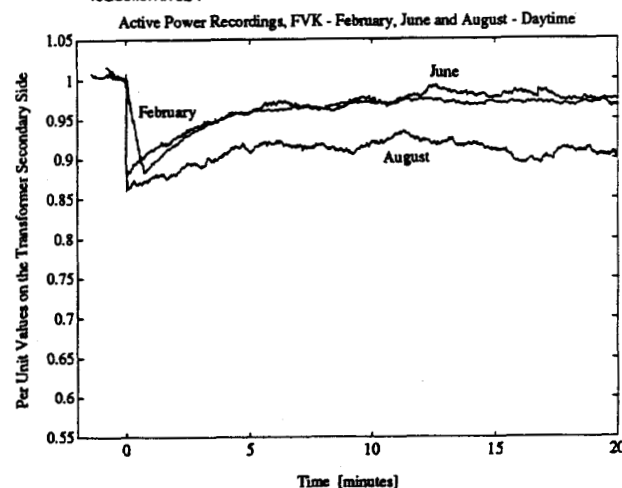
Figure 4.5a. Active power recordings after a voltage reduction in FVK

In Figure 4.5 the influence of the time of the year is presented for load FVK in comparison with the influence of the time of the day shown in Figure 4.4.
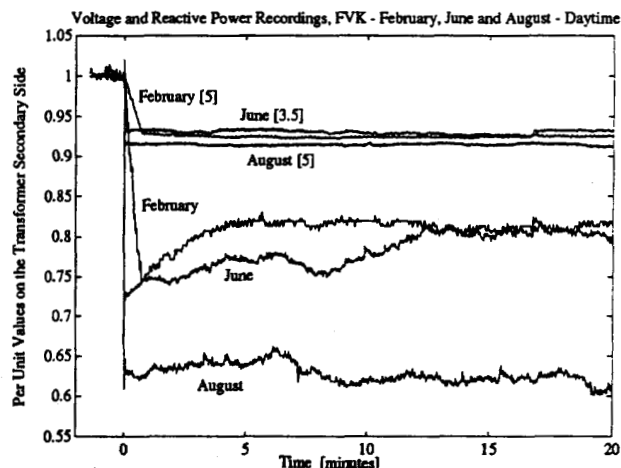
Figure 4.5b. Voltage and reactive power recordings after a voltage reduction in FVK

4.2 Specific Load Model Structure and Parameter Identification

The structure of a load model describing the temporary load-voltage characteristic is derived first. Then the parameters describing the behaviour of the different composite loads have to be identified. For the voltage ramp and step-change responses, Figures 4.4 and 4.5, a first order model seems to be sufficient. General aspects of this recovery response were described in Section 2.

The model structure which is similar for both the active and reactive power is chosen as form (14), (15) with exponential functions (16), (17)

$$T_p \frac{dP_r}{dt} + P_r = N_p(V) \; ; \; N_p(V) = P_0 \left(\frac{V}{V_0}\right)^{a_s} - P_0 \left(\frac{V}{V_0}\right)^{a_t} \quad (26)$$

$$P_d = P_r + P_0 \left(\frac{V}{V_0}\right)^{a_t} \quad (27)$$

$$T_q \frac{dQ_r}{dt} + Q_r = N_q(V) \; ; \; N_q(V) = Q_0 \left(\frac{V}{V_0}\right)^{\beta_s} - Q_0 \left(\frac{V}{V_0}\right)^{\beta_t} \quad (28)$$

$$Q_d = Q_r + Q_0 \left(\frac{V}{V_0}\right)^{\beta_t} \quad (29)$$

where

a_s = steady state active load-voltage dependence
a_t = transient active load-voltage dependence
β_s = steady state reactive load-voltage dependence
β_t = transient reactive load-voltage dependence
P_0 = active power consumption at pre-fault voltage (MW)
P_d = active power consumption model (MW)
P_r = active power recovery (MW)
Q_0 = reactive power consumption at pre-fault voltage (MVar)
Q_d = reactive power consumption model (Mvar)
Q_r = reactive power recovery (Mvar)
T_p = active load recovery time constant (s)
T_q = reactive load recovery time constant (s)
V = supply voltage (kV)
V_0 = pre-fault of supply voltage (kV)

As discussed in Section 2, the model consists of a steady-state part and a dynamic part; for real power loading those are

$$P_s(V) = P_0 \left(\frac{V}{V_0}\right)^{a_s} \text{ and } P_t(V) = P_0 \left(\frac{V}{V_0}\right)^{a_t} \text{ respectively.}$$

The model will be shown valid for both the ramp and the step-change of the supply voltage, when applied to a composite load, including some electric heating.

From Figure 2.2, the expression

$$PRF = \frac{\Delta P_t - \Delta P_s}{\Delta P_t} = \frac{P_0(V_+/V_0)^{a_s} - P_0(V_+/V_0)^{a_t}}{P_0 - P_0(V_+/V_0)^{a_t}} \approx \frac{a_t - a_s}{a_t} \quad (30)$$

can be identified as an active load recovery factor (PRF). A corresponding factor (QRF) can be defined for the reactive power.

There are alternative ways to use the data recorded during the field measurements, for estimating the parameters in (26)–(29). The parameters estimated accurately depend on the sampling period used for the identification. Using a longer sampling period emphasizes the low frequency properties of the model; the influence of random load demand variations is significant, which makes the identification less accurate. On the other hand, the use of a small sampling period emphasizes the high frequency properties, and the influence of random load demand variations becomes negligible. These conditions apply particularly to ramps and step-changes. To investigate the influence of the proportions of the time series recorded on the estimated parameters, different intervals were used for the parameter identification of the step and ramp variations. Intervals 2, 4, 7, 15, and 30 minutes were used for the step, and double these values for the ramp. Using around 15 minutes of the time series recorded provided the most accurate result; the power recovery had become stabilized and the random load demand did not vary too much. The $a_t(\beta_t)$ parameter can be estimated from the step-change with very high accuracy. For a_s and T_p (β_s and T_q), the accuracy is obviously less, due to the influence of random load demand variations.

Curve fitting with the least-square method was used for the parameter value identification. V_0, P_0 and Q_0 were chosen as the values of V, P and Q, respectively, just before the step or ramp. For the step-changes, $a_t(\beta_t)$ was derived from the value of V_+ and $P_+(Q_+)$, immediately after the step as

$$a_t = \frac{\log \frac{P_+}{P_0}}{\log \frac{V_+}{V_0}} \; ; \; \beta_t = \frac{\log \frac{Q_+}{Q_0}}{\log \frac{V_+}{V_0}} \qquad (31)$$

Then a_s and $T_p(\beta_s$ and $T_q)$ were obtained by using the non-linear least-square method. Similarly, the parameters can be estimated from the ramp response; $a_t(\beta_t)$ are derived from final values and a_s and $T_p(\beta_s$ and $T_q)$ using the non-linear least-square method.

4.3 Results from Field Measurements

The parameters, describing the temporary load-voltage characteristic, a_s, a_t and $T_p(\beta_s, \beta_t$ and $T_q)$, for the voltage ramps and step-changes applied at the two substations, are shown in Tables I and II, for daytime, evening and night loads.

The models derived and recordings are seen to agree closely. In Figure 4.6, curve 1 shows the real power recorded at FVK, curve 2 the modelled power, curve 3 the steady-state load-voltage characteristic and curve 4 the transient load-voltage characteristic. More details are given in [16]. Tables I and II show clearly that it is necessary to use different load model parameter values for different times of the day and different days of the year. The load consumption response varies for different types of load composition.

Active Power during a Voltage Reduction in FVK 1991-02-19, Daytime
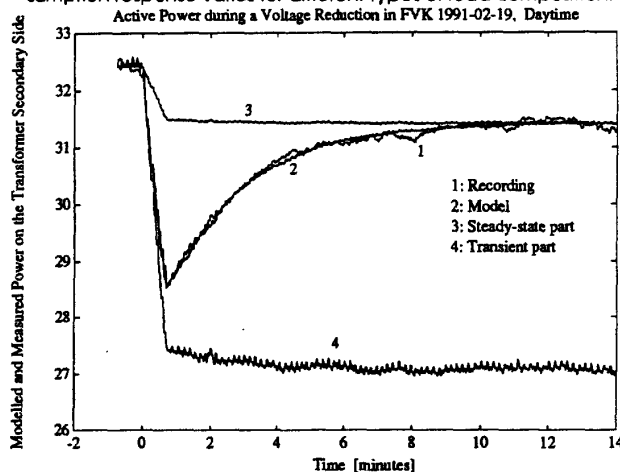
Figure 4.6. Model and recording of active power after a voltage ramp in FVK; February; daytime.

Table I: Active power load model parameter estimation results for ramps and steps in the supply voltage.

Area	Month	Time	$P_0[MW]$	a_s	a_t	$T_p[s]$	PRF
FVK	Feb	Day	32.28	0.38	2.26	127.6	0.822
FVK	Feb	Evening	36.15	0.54	2.20	143.5	0.730
FVK	Feb	Night	27.98	0.17	2.46	140.6	0.924
FVK	June	Day	20.06	0.23	1.77	202.1	0.860
FVK	June	Evening	16.21	0.44	1.78	148.7	0.734
FVK	June	Night	14.90	0.17	1.83	186.4	0.897
FVK	Aug	Day	11.66	0.90	1.62	218.3	0.429
FVK	Aug	Evening	9.13	0.58	1.58	211.4	0.616
FVK	Aug	Night	–	–	–	–	–
SLA	Feb	Day	15.41	0.31	1.85	163.4	0.819
SLA	Feb	Evening	15.74	0.45	1.99	139.2	0.759
SLA	Feb	Night	10.25	0.05	2.05	159.6	0.970
SLA	June	Day	10.38	0.57	1.64	164.7	0.633
SLA	June	Evening	7.41	0.79	1.60	363.8	0.490
SLA	June	Night	6.40	1.04	1.77	146.7	0.392
SLA	Aug	Day	9.76	0.83	1.57	351.6	0.457
SLA	Aug	Evening	7.48	1.09	1.50	352.0	0.260
SLA	Aug	Night	5.38	1.39	1.56	83.0	0.105

Table II: Reactive power load model parameter estimation results for ramps and steps in the supply voltage.

Area	Month	Time	$Q_0[Mvar]$	β_s	β_t	$T_q[s]$	QRF
FVK	Feb	Day	5.56	2.68	5.22	75.3	0.437
FVK	Feb	Evening	6.48	2.10	4.96	114.7	0.504
FVK	Feb	Night	3.77	2.40	6.73	110.4	0.566
FVK	June	Day	3.97	1.72	4.76	1024.8	0.597
FVK	June	Evening	3.49	4.02	4.90	55.5	0.148
FVK	June	Night	2.28	4.38	6.32	112.5	0.250
FVK	Aug	Day	3.09	5.18	5.27	47.9	0.014
FVK	Aug	Evening	2.81	5.08	5.43	62.1	0.050
FVK	Aug	Night	–	–	–	–	–
SLA	Feb	Day	5.23	3.53	4.18	131.7	0.130
SLA	Feb	Evening	4.69	4.03	4.57	47.9	0.096
SLA	Feb	Night	2.68	4.99	6.65	22.9	0.188
SLA	June	Day	6.09	3.94	4.80	167.8	0.150
SLA	June	Evening	3.94	4.84	5.03	73.0	0.031
SLA	June	Night	3.06	5.20	5.61	17.8	0.058
SLA	Aug	Day	5.84	4.10	4.64	24.1	0.097
SLA	Aug	Evening	3.86	4.59	5.07	0.1	0.076
SLA	Aug	Night	2.91	5.34	5.45	3.4	0.016

In special situations, model simplifications can be used. As described in Section 2, if the indices a_t and a_s are close, a simpler cascade model (Figure 2.5(b)) is applicable. The field measurements used here show that when there is a small amount of heating compared to industrial load (SLA area), there is almost no recovery. In this case, a static load model would suffice.

5 Conclusions

This paper has presented a methodology for dynamic load modelling oriented to large disturbance stability studies. The motivation has been towards voltage stability analysis, but the techniques are equally applicable to time-scales for transient (angle) stability. The models can be expressed as higher-order or normal (first-order higher dimensional) form differential equations with special structure related to steady-state and transient load response. There is also a convenient block diagram representation in terms of nonlinear functions and a linear transfer function. The parameters of the model can be identified from field measurement data using a combination of closed form formulae (for step and ramp responses) and least squares curve fitting.

Based on field measurements the identification of a load model with recovery in the time scale of minutes has been carried out; the recovery largely originated from thermostat controlled heating devices. The effect of (faster) recovery in electrical motors [9] and due to tap-changers at higher voltage buses has not been

deait with. This requires measurements on other time-scales and voltage levels. Shackshaft et. al. [17] has already made load recovery recordings on a time-scale of seconds where motor load behaviour is significant. An analytical discussion of how various load devices have their recovery behaviour captured by the model presented in Section 2 is given in [13].

Even within the scope of the present experimental project, there are some refinements. It is difficult to deal with the random variations in power demand. There is also the problem of load drift and change in composition; it is impossible to repeat a recording on the same load composition for different applied voltages. More sophisticated measurements and signal processing such as stochastic parameter identification could help [20].

Certainly, this will be the case when more complicated forms for $P_x(\cdot)$ and $P_f(\cdot)$ are used which require more coefficients. The measurement techniques in [16] also provide responses to sinusoidal and pseudo-random noise voltage signals; these should help provide more detailed models.

The load recovery measured in the above work includes the aggregate effect of normal domestic and industrial load. This includes electrical home heating as a major source of seasonal variation. The load modelling project at Chalmers University includes investigations of load response on these and other devices to compare with the aggregate responses [9, 15, 22].

The thesis by Karlsson [16] considers other aspects of load response with respect to physical behaviour. For instance, the active and reactive recovery responses are related. For the loads considered here, the reactive power recovery originates from increased reactive losses in the distribution system following active power recovery.

The modelling methodology has already yielded insights into the nature of dynamic voltage phenomena and their control. The initial jump in load (see Figure 2.2) of course gives temporary relief to the system following a voltage drop. The recovery restores load. The study of implications for understanding dynamic voltage stability has begun in [12–14]. The thesis [16] has looked at blocking strategies based on dynamic load type for OLTCs to avoid voltage collapse. It also seems reasonable to consider recovery models in transient (angle) stability studies. As discussed in [13], recovery models can be in principle identified in a time scale of seconds including the effect of motor load [17].

In principle the effect of OLTCs can also be incorporated into the load model evaluated at higher voltages, but this requires more intrusive field measurement techniques.

Acknowledgement

References

[1] G.J. Berg, "Power-system load representation", Proc. IEE, Vol. 120, No. 3, March 1973, pp. 344-348.

[2] T. Ohyama et. al., "Voltage dependence of composite loads in power systems", IEEE Trans. on Power Apparatus and Systems, Vol. PAS-104, No.11, November 1985, pp. 3064-3073.

[3] IEEE Task Force Report, "Load representation for dynamic performance analysis", IEEE Power Engineering Society Paper 92WM 126-3 PWRD.

[4] A.A. Fouad and V. Vittal, "The transient energy function method", Int. J. of Electrical Power and Energy Systems, Vol. 10, No. 4, October 1988, pp. 233-246.

[5] R.H. Craven and M.R. Michael, "Load representation in the dynamic simulation of the Queensland power system", J. of Electrical and Electronics Engineering, Vol. 3, No. 1, 1983, pp. 1-7.

[6] I.A. Hiskens and D.J. Hill, "Energy functions, transient stability and voltage behaviour in power systems with nonlinear loads", IEEE Trans. on Power Systems, Vol. 4, pp. 1525-1533, November 1989.

[7] Y. Mansour, (ed.), Voltage stability of power systems: Concepts, Analytical Tools, and Industry Experience, IEEE Task Force Report, Publication 90TH 0358-2-PWR.

[8] K. Walve, "Modelling of power system components at severe disturbances", CIGRE report 38-18, 1986.

[9] D. Karlsson and T. Pehrson, "A dynamic power system load model and methods for load model estimation", Technical Report 22L, Department of Electrical Power Systems, Chalmers University of Technology, Sweden, 1985.

[10] A. Edström and K. Walve, "Dynamisk Lastmodell", Technical Report EKC – Vattenfall, June 1987.

[11] D.J. Hill, "A simple load model with recovery for power system stability studies", University of Newcastle Technical Report EE9133, April 1991.

[12] P.-A. Löf, "Study of Long-term voltage stability in electric power systems", Licentiate Thesis, Royal Institute of Technology, Sweden, April 1991.

[13] D.J. Hill, "Nonlinear dynamic load models with recovery for voltage stability studies", IEEE Power Engineering Society, Publication 92WM 102-4 PWRS.

[14] D.J. Hill, I.A. Hiskens and D. Popovic, "Stability analysis of load systems with recovery dynamics", submitted to IEEE 1993 Winter Meeting.

[15] D. Karlsson, K. Lindén, I. Segerqvist and B. Stenborg, "Temporary load/voltage characteristics for voltage stability studies – field measurements, laboratory measurements, and simulations", to appear CIGRE SC38, Paris 1992.

[16] D. Karlsson, "Voltage stability simulations using detailed models based on field measurements", PhD Thesis, Chalmers University of Technology, Sweden, June 1992.

[17] G. Shackshaft, O.C. Symons and J.G. Hadwick, "General – purpose model of power system loads", Proc. IEE, Vol. 24, No. 8, August 1977.

[18] D.J. Hill and I.A. Hiskens, "Dynamic analysis of voltage collapse in power systems", to appear 31st Conference on Decision and Control, Tuscon, Arizona, December 1992.

[19] T. Kailath, Linear Systems, Prentice-Hall, New Jersey, 1980.

[20] S. Graebe and T. Bohlin, "Identification of Nonlinear Stochastic Grey Box Models: Theory and Implementation and Experiences", Preprints 4th IFAC International Symposium on Adaptive Systems in Control and Signal Processing, Grenoble, France, pp. 401–406.

[21] G.C. Goodwin and R.L. Payne, Dynamic System Identification: Experiment Design and Data Analysis, Academic Press, New York, 1977.

[22] J. Näslund, "The load-voltage dependence of home heating appliances", Diploma Thesis 91-03 1991, Dept. of Electrical Power Systems, Chalmers University of Technology. (In Swedish).

Biography

Daniel Karlsson received his Master's degree (Electrical Engineering) and the degree of Licentiate of Engineering (Electrical Engineering) from Chalmers University of Technology, Sweden in 1982 and 1985 respectively. In 1992 he received the Ph.D degree in Electrical Engineering from Chalmers University of Technology, Sweden. Since 1985 he has been an analysis engineer at the Power System Analysis Group within the Operation Department of Sydkraft, the largest private power company in Sweden. His work has been in the protection and power system analysis area and the research has been on the voltage stability and collapse phenomenon with emphasis on the influence of loads, on-load tap-changers and generator reactive power limitations.

DAVID J. HILL received the Ph.D. degree in Electrical Engineering from the University of Newcastle, Australia in 1976. He is currently Professor in the Department of Electrical and Computer Engineering at the University of Newcastle, occupying the Pacific Power Chair. During 1986 he was a Guest Professor in the Department of Automatic Control, Lund Institute of Technology, Sweden where he developed research projects in power system analysis and control. His research interests are mainly in nonlinear systems and control engineering with application to power plant and systems.

Discussion

M. K. Pal: As stated in the introduction, the load modeling work reported in the paper was motivated by current work in voltage stability. Our comments, likewise, apply mainly to voltage stability analyses. In vast majority of voltage stability analyses, a higher order dynamic load model is not really necessary. Voltage stability is determined by overall dynamic behavior of the load. The overall response speed of aggregate load is generally slow. Therefore, a first order model should be sufficient. The authors basically seem to agree with this contention. Based on field measurements, they have also identified a first order load model for loads with slow recovery time. The significant features of the aggregate load response as observed by the authors in laboratory and field tests are also what one would expect from the known behavior of the individual load devices and/or from well established mathematical models of these devices.

A higher order model might be appropriate in a general stability analysis that encompasses voltage stability. When the individual devices are large and form a significant part of the total load, a first order model may not be adequate to represent these devices. This would be especially true if these loads have complex dynamics that significantly affect stability results. In such situations it would be prudent to use rigorously derived detailed models for these devices, rather than rely on higher order aggregate models derived from field tests. Aggregate models are useful when a model is needed and nothing else is available, or when the actual form of the model or parameter values are relatively unimportant. In our discussion we therefore concentrate on first order model.

It would be instructive to compare the models of the paper with that used in [A-B], the general form of which is shown in equation (1).

$$T_{Lp}\dot{G} = P(V) - V_o^2(V/V_o)^n G \qquad (1)$$

with $n \geq 1.0$, for the real power, and similarly for the reactive power.

The model given by (1) has characteristics similar to the first order model discussed through much of the paper. Although the model is referred to as a generic aggregate load model, it is in a form that naturally describes several common dynamic load types, e.g. impedance loads rendered dynamic by LTCs, approximate model (the slip model) of induction motors, etc. Actually, models of all known dynamic load devices derived from physical laws show overall response behavior similar to that of (1). There is no reason why the overall aggregate behavior should be any different. Physical reasoning suggested the limit imposed on the value of n. Actual values of the parameters are not important for providing insights and explain the various phenomena in voltage stability.

Differentiating (1), and after some manipulations, the above load model can be reduced to the form of equation (3) or (5) of the paper. Equation (3) of the paper is, therefore, an alternative form of (1). (Yes, (1) looks too simple to deserve serious attention; but looks can be deceiving.) However, equation (3) would be awkward to handle in numerical simulations, since it would require transformation to another form, e.g., equation (7) or (14). This would tend to suppress the fact that the physical validity of the model is dependent on the parameter values and that any anomaly in parameter values would have to be identified.

As pointed out in [C], in the authors' formulation it is easy to assign inappropriate values to the parameters, so that stability conclusions from static and dynamic analyses conflict when they should not. For example, it has been shown in [C] for a specific load, and in [B] for a number of different load types using actual dynamic models, that for constant source voltage, the stability results from static and dynamic analyses are identical. In other words, when the source voltage can be assumed to be constant, voltage stability results are independent of load model as long as the model is physically valid.

Note that in the paper's special case where the steady-state and transient load functions are related by constant scaling, the stability results can be anomalous, depending on the numerical value of C chosen. For example, with $C = 1.0$, stability is always maintained. (No indication of the range of values of C is given in the paper.)

The generic load model suggested in [D] is also of the form of equation (1), except that the correct limits of the transient parameter values have not been recognized. The consequences are discussed in [E].

In voltage stability studies the objective is to assess stability status, and devise and evaluate methods for improving stability. Actual voltage dynamic performance is rarely of any concern. This justifies the use of an aggregate model that captures the essential features of the load dynamics affecting voltage stability. The model must however be physically justified. It should also be reasonably simple and convenient for computational purposes.

The dynamic load model derived in this and the previous paper [13] is more complex than it need be. As has been pointed out in [C], the model uses variables which are not true state variables. This requires transformation of variables before the model can be used in actual computations.

While dynamic concepts and dynamic load models are necessary to provide insights into the problems and explain various phenomena, actual dynamic system analyses for voltage stability are rarely necessary, since the same answer as from a dynamic analysis can be obtained from a steady-state analysis [A-B]. In specific situations when dynamic analyses are deemed necessary, the use of detailed models of the individual load devices should be considered. The use of a generic aggregate load model would be inappropriate in such situations [B].

In response to the authors' conclusions, we would like to comment that the voltage stability problem is now well understood. Cost-effective solutions can be devised for most utility systems, although their general acceptance and implementation will require some time. More exotic load models are not likely to yield additional insights into the subject.

References

[A] M. K. Pal, "Voltage Stability Conditions Considering Load Characteristics," IEEE Trans. on Power Systems, Vol. 7, No. 1, pp. 243–249, Feb. 1992.

[B] M. K. Pal, "Voltage Stability: Analysis Needs, Modelling Requirement and Modelling Adequacy," to appear in IEE (UK) Proc. C, Gen. Trans. & Distrib.

[C] M. K. Pal, Discussion of reference [13] of the paper.

[D] W. Xu and Y. Mansour, "Voltage Stability Analysis Using Generic Dynamic Load Models," IEEE PES Winter Meeting, Jan. 31–Feb. 3, 1993, Columbus, OH, 93 WM 185-9-PWRS.

[E] M. K. Pal, Discussion of [D].

William W. Price (GE Power Systems Engineering, Schenectady, NY): This paper presents a very thorough and interesting discussion of dynamic load models and is a valuable contribution to this field. Would the authors please clarify equation (3)? I

believe it is intended that there be a "dot" over the last V as well as over the first P_d. Also, it may be of interest that the IEEE Task Force on Load Representation for Dynamic Performance is preparing a set of recommended load models. A dynamic model of the following form has been proposed:
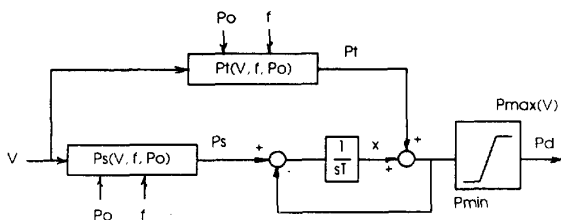
Except for the addition of the limit on the output and the frequency dependency, this model is mathematically equivalent to the authors' first-order model as shown in figure 2.5(a) of the paper. The form is slightly different in order to retain the steady-state load characteristic (P_S) explicitly in the model rather than the function $N = P_S - P_t$ which the authors include. Would the authors care to comment on the desirability of including this type of model as a recommended model for dynamic performance analysis? In particular, do they have any strong objections to the use of the above form rather than their figure 2.5(a)?

Manuscript received February 25, 1993.

S. Casper, L-Y. Xu, and **C. O. Nwankpa** (ECE Department, Drexel University, Philadelphia, PA):

The authors should be commended for their interesting paper on applying parameter identification techniques to dynamic load models for large voltage disturbances. We agree with the authors on "... the importance of accurate load modeling in voltage stability analysis" which is the motivation of this work. The discussors will appreciate authors' comments on the following.

The load model closely describes load response to a voltage step or ramp immediately after the voltage disturbance and for several minutes representing the recovery time. One concern we have about this model is how well does it model a system with time-varying load composition which is an accurate representation of reality where there is significant customer switchings. If the authors' model is not applicable to this situation, what suggestions do you have on addressing this problem? In addition, the tests in the paper were described for "...composite load, including some electric heating." How does this model hold for load compositions of various types? Can this model be used for a generic load composition or for specific loads of one particular composition?

Manuscript received March 1, 1993.

Daniel Karlsson, David J. Hill: We thank the discussers for their valuable comments and questions. Many of these constitute contributions to the subject of the paper.

William W. Price:

There is a dot over the last V as well as over the first P_d in equation (3). These two dots are not presented as clearly as the dots in equation (1).

It is correct that the block diagram in Figure 2.5(a) and the block diagram in this discussion are mathematically equivalent. It would be useful to know the source of the latter diagram. In Figure 2.5(a), the form of the block diagram avoids any feedback signal from P_d. In equation (26) of the paper, P_r can be identified as x in the block diagram of Mr. Price's discussion. The choice of form of the block diagram is more a matter of taste, and depends on the purpose of the diagram. We do not have "any strong objections" to the use of the alternative block diagram proposed.

M. K. Pal:

The authors generally agree with the opening remarks which echo ideas expressed in references [11-16]. It is also pleasing to see that Dr. Pal now accepts the value of aggregate load models in contrast to earlier comments [C].

Model (1) in the discussion (which generalises that in [A] where $P(V)=P_0$ and n=2) is actually a special case of the more general class of models discussed in [13], i.e.

$$\dot{P}_d + f(P_d, V) = g(P_d, V)\, \dot{V} \qquad (c1)$$

Similarly, model (3) in the paper and the model in [D] are all different special cases of this class. These models share some common behaviour, but differ in detail. Some results connecting these various aggregate models to particular device characteristics have been reported [13, C], but the comment that models of all known dynamic load devices derived from physical laws show overall response behaviour similar to that of (1) in the discussion has not been justified.

The authors have never suggested using the form (3) in numerical simulations; the results of references [12, 14, 16] have all used the normal form (7)-(8); the transformation between input-output and state-space forms is trivial.

The issue of static vs dynamic stability conclusions (which is partly a matter of semantics) certainly was not fully resolved in [13, C]; it is an unnecessary distraction here. The authors do not agree with Dr. Pal that "... actual dynamic system analyses for voltage stability are rarely necessary, since the same answer as from a dynamic analysis can be obtained from a steady-state analysis.."

Even less do we agree "that the voltage stability problem is now well understood". This opinion is derived from practical and theoretical curiosity.

A complete response to Dr. Pal is not possible because some of the references in his discussion are not yet published.

S. Casper, L-Y. Xu, C. O. Nwankpa:

The disussers first question is about how well the proposed load model models a system with time-varying load composition, which originates from customer switchings. The answer is that the structure of the model is applicable for all the compositions investigated. The parameter values, however, differ for different times of the day and different times of the year. This means that the load model structure holds for time-varying load compositions, but the parameters have to be adjusted.

The second question is about how well the load model holds for load compositions of different types. The field measurements were performed in two different substations in the South of Sweden for different times of the year and different times of the day. One of the substations was feeding an "extremely" residential load composition, consisting of a village with mainly one-family houses and no industry at all (about 10 000 households). The other substation was feeding a slightly smaller village including a quite big industry. The load model is accurate for all the recordings from these two substations. The active power recovery largely originates from thermostat controlled heating devices, which is a large part of the load during winter. The load model does not include induction machine dynamics or any other short term dynamics (time constants less than 10 seconds). It is the opinion of the authors that the structure of the proposed load model is valid for residential and commercial load compositions including some electrical heating. Induction machines and other specific load devices with certain characteristics have to be modelled separately, if they are a large part of the total load or if their behaviour is significant for the study.